Field and dispersion properties of subwavelength-diameter hollow optical fiber

Chujun Zhao[1], Zhixiang Tang[1], Yunxia Ye[1], and Dianyuan Fan[1], Liejia Qian[2], Shuangchun Wen[3], and Guanghui chen[4]

[1]*Shanghai Institute of Optics and Fine mechanics, Chinese Academy of Science, Shanghai 201800, China*
[2]*Department of Optical Science and Engineering, Fudan University, Shanghai 200433, China*
[3]*School of Computer and Communication, Hunan University, Changsha 410082, China*
[4]*Electronics Technology Group Corporation No.23 Research Institute, Shanghai 200437, China*
c_j_zhao@yahoo.com.cn

Abstract: We have investigated the basic properties of subwavelength-diameter hollow optical fiber with exact solutions of Maxwell's equations. The characteristics of modal field and waveguide dispersion have been studied. It shows that the subwavelength-diameter hollow optical fibers have interesting properties, such as enhanced evanescent field, local enhanced intensity in the hollow core and large waveguide dispersion that are very promising for many miniaturized high performance and novel photonic devices.

References and links

1. L. M. Tong, R. R. Gattass, J. B. Ashcom, S. L. He, J. Y. Lou, M. Y. Shen, I. Maxwell, and E. Mazur, "Subwavelength-diameter silica wires for low-loss optical wave guiding," Nature **426**, 816-819 (2003).
2. L. M. Tong, J. Y. Lou, and E. Mazur, "Single-mode guiding properties of subwavelength-diameter silica and silicon wire waveguides," Opt. Express **12**, 1025-1035 (2004)
http://www.opticsinfobase.org/abstract.cfm?URI=oe-12-6-1025.
3. J. Y. Lou, L. M. Tong, and Z. Z. Ye, "Dispersion shifts in optical nanowires with thin dielectric coatings," Opt. Express **14**, 6993-6998 (2006)
http://www.opticsinfobase.org/abstract.cfm?URI=oe-14-16-6993.
4. L. M. Huang, H. T. Wang, C. Y. Hayashi, B. Z. Tian, D. Y. Zhao and Y. S. Yan, "Single-strand spider silk templating for the formation of hierarchically ordered hollow mesoporous silica fibers," J. Mater. Chem. **13**, 666–668 (2003).
5. D. Penman, "Spider silk delivers finest optical fibres," New Scientist **12** (2003).
6. E. Karadeniz and P. Kornreich, "Intercore-cladding uniaxial dielectric thin film optical fibers," Opt. Eng. **45**, 085001-1-10 (2006).
7. U. Schröter and A. Dereux, "Surface plasmon polaritons on metal cylinders with dielectric core," Phys. Rev. B **64**, 125420 (2001).
8. A. W. Snyder, and J. D. Love, *Optical waveguide theory* (Chapman and Hall, New York, 1983).
9. V. R. Almeida, Q. Xu, C. A. Barrios, and M. Lipson, "Guiding and confining light in void nanostructure," Opt. Lett. **29**, 1209-1211 (2004).
10. G. S. Wiederhecker, C. M. B. Cordeiro, F. Couny, F. Benabid, S. A. Maier, J. C. Knight, C. H. B. Cruz and H. L. Fragnito,"Field enhancement within an optical fibre with a subwavelength air core," Nature Photonics **1**, 115-118 (2007).

1. Introduction

Dielectric optical waveguides with widths or diameters from micrometers to millimeters have got successful applications in many fields such as optical communication, optical sensing and optical power delivery systems [1]. Many applications benefit from minimizing the width of the waveguides, but fabricating low-loss optical waveguides with subwavelength diameters remains challenging because of high precision requirement. Recently, several types of dielectric submicrometer and nanometer diameter wires of optical qualities have been obtained [1-3]. These wires, with diameters smaller than a micrometer, are tens to thousands

times thinner than the commonly used micrometer diameter waveguides. They can be used as air-clad wire-waveguides with subwavelength-diameter cores, and building blocks in the future micro- and nano- photonic devices [2]. These fibers have solid cores and the guiding properties of the waveguides have been adequately studied. However, for the subwavelength-diameter fiber with a hollow core, the guiding characteristics have not been discussed. For experiments, Yushan Yan and a team of engineers from the University of California at Riverside gave the spider's silk thread a glassy coating, and then extracted the silk by baking. They soon expect to be able to make hollow fibers with cores just two nanometers wide or 50,000 times thinner than a human hair [4, 5]. So it is clear that subwavelength-diameter hollow optical fiber (SHOF) will be available in the near future and the fiber offers opportunities for a lot of miniaturized high performance and novel photonic devices. In this paper, based on exact solutions of Maxwell's equations and numerical calculations, the basic guiding properties of subwavelength-diameter hollow wires have been studied. We choose fused silica (SiO_2) as typical dielectric materials for our simulation.

2. Mathematical model for SHOF

The refractive index profile is schematically illustrated in Fig. 1. A long straight SHOF is a cylindrical structure of rotational symmetry involving three regions in the cross section: a hollow core with radius a, dielectric region with radius b, and the infinite air cladding. Refractive indices of the core, dielectric region and outer cladding are assumed to be n_1, n_2, and n_3, respectively. Translational invariance in the z direction implies that there exist single-spatial-frequency solutions proportional to $\exp(j(wt-\beta z))$, where w is the angular frequency and β is the longitudinal propagation constant [6-8].
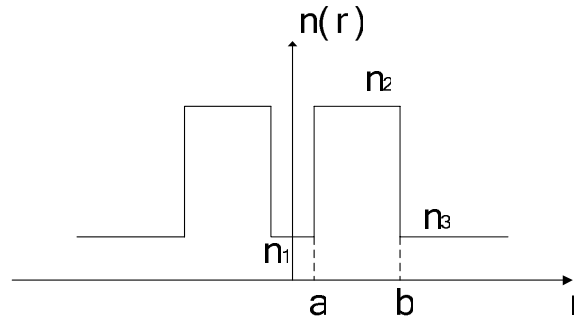

Fig. 1. The cross-section and parameters of the SHOF.

The z components of the field, E_z and H_z, satisfy the following Helmholtz equation in the homogeneous sections in which refractive index is constant,

$$[\frac{1}{r}\frac{\partial}{\partial r}(r\frac{\partial}{\partial r})+\frac{1}{r^2}\frac{\partial^2}{\partial \phi^2}+(k_0^2 n^2 - \beta^2)]\begin{pmatrix} E_z \\ H_z \end{pmatrix} = 0 , \qquad (1)$$

where $k_0=wc=w(\mu_0\varepsilon_0)^{1/2}$ is the free space wave number, ε_0 is the free-space permittivity, and c is the speed of light. For $k_0^2 n^2 - \beta^2 > 0$, these equations predict propagating waves with the Bessel functions J_m and Y_m as solutions, and for $k_0^2 n^2 - \beta^2 < 0$, they predict exponentially decaying or growing fields with modified Bessel functions I_m and K_m as solutions. Longitudinal field components can now be written as

$$E_z = \begin{cases} AI_m(u_1 r)f_c, & 0<r<a \\ [BJ_m(u_2 r)+CY_m(u_2 r)]f_c, & a<r<b \\ DK_m(u_3 r)f_c, & r>b \end{cases} , \qquad (2)$$

$$H_z = \begin{cases} A'I_m(u_1 r)f_s, & 0 < r < a \\ [B'J_m(u_2 r) + C'Y_m(u_2 r)]f_s, & a < r < b \ , \\ D'K_m(u_3 r)f_s, & r > b \end{cases} \qquad (3)$$

where $\quad u_1 = \sqrt{\beta^2 - k_0^2 n_1^2} \quad$, $\quad u_2 = \sqrt{k_0^2 n_2^2 - \beta^2} \quad$, $\quad u_3 = \sqrt{\beta^2 - k_0^2 n_3^2} \quad$,

$f_c = \cos(m\phi + \varphi_m)\exp[j(wt - \beta z)]$, $f_s = \sin(m\phi + \varphi_m)\exp[j(wt - \beta z)]$. The transverse field components are obtained from the following equations:

$$E_r = -\frac{j}{k_0^2 n^2 - \beta^2}(\beta\frac{\partial E_z}{\partial r} + \frac{w\mu_0}{r}\frac{\partial H_z}{\partial \phi}),$$

$$E_\phi = -\frac{j}{k_0^2 n^2 - \beta^2}(\frac{\beta}{r}\frac{\partial E_z}{\partial \phi} - w\mu_0\frac{\partial H_z}{\partial r}),$$

$$H_r = -\frac{j}{k_0^2 n^2 - \beta^2}(\beta\frac{\partial H_z}{\partial r} - \frac{w\varepsilon_0 n^2}{r}\frac{\partial E_z}{\partial \phi}),$$

$$H_\phi = -\frac{j}{k_0^2 n^2 - \beta^2}(\frac{\beta}{r}\frac{\partial H_z}{\partial \phi} + w\varepsilon_0 n^2\frac{\partial E_z}{\partial r}).$$

Applying boundary conditions at $r=a$ and $r=b$, a system of eight linear homogeneous equations is obtained that is satisfied by the eight coefficients. The system admits a nontrivial solution only in case its determinant is zero. The propagation constant β is determined by the condition that the determinant of the system of linear equations shall vanish:

$$\det[M(\beta)]=0, \qquad (4)$$

where M is the resulting matrix of the system of equations. Usually, subwavelength-diameter optical fibers are designed and desired for working as single-mode waveguides, therefore, here we consider the fundamental modes and thus set $m=1$ in Eqs. (2) and (3). With propagation constants obtained by numerically solving Eq. (4), the group velocities(v_g) and waveguide dispersions(D_w) can be obtained as [3]:

$$v_g = \frac{dw}{d\beta} = -\frac{2\pi c}{\lambda^2}\frac{d\lambda}{d\beta} , \qquad (5)$$

$$D_W = \frac{d(v_g^{-1})}{d\lambda} . \qquad (6)$$

The power flow (power density) along the z direction in cylindrical coordinates is given by

$$S_z = \frac{1}{2}\Re[E_r H_\phi^* - E_\phi H_r^*]. \qquad (7)$$

We assume that the index of the air (n_1 and n_3) is 1.0, and use the following Sellmeier-type dispersion formula (at room temperature) to obtain the refractive indices of the dielectric materials for fused silica (SiO$_2$)

$$n^2 - 1 = \frac{0.6961663\lambda^2}{\lambda^2 - (0.0684043)^2} + \frac{0.4079426\lambda^2}{\lambda^2 - (0.1162414)^2} + \frac{0.8974794\lambda^2}{\lambda^2 - (9089616)^2} , \qquad (8)$$

where the unit of λ is μm.

3. Results and discussion

For the convenience, we use normalized propagation constant B to characterize the fiber and it is defined by $B = (\beta^2 - k_0^2 n_3^2)/(k_0^2 n_2^2 - k_0^2 n_3^2)$. If the hollow region radius is set to be 10 nm and the dielectric region radius varies, the B parameter increases with increasing b and decreases with increasing wavelength, as shown in Fig. 2(a). If the dielectric region radius is set to be 100 nm and the hollow region radius varies, the B parameter decreases with increasing a and increasing wavelength, as shown in Fig. 2(b). It can be concluded that the SHOF with thicker dielectric region has higher parameter B.
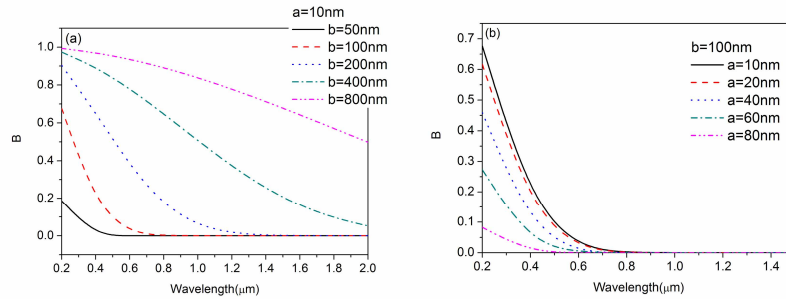

Fig. 2. Variation of B with wavelength for SHOF with (a) different b; (b) different a.

Normalized electric components of the fundamental mode for SHOF at 633 nm wavelength are shown in Fig. 3, which shows the different field profiles for SHOFs with different dielectric region radius b ranging from 100 nm to 800 nm and fixed hollow core size a=10 nm. When the radius of dielectric region reduces to a certain degree, the field begins to extend to a far distance with considerable amplitude, indicating that the majority of the field is no longer tightly confined inside or around the SHOFs. Compared with the subwavelength-diameter optical fiber without the hollow region [2], the SHOFs show the similar behavior in the region $r>b$. However, for the central region, the SHOFs behave differently.
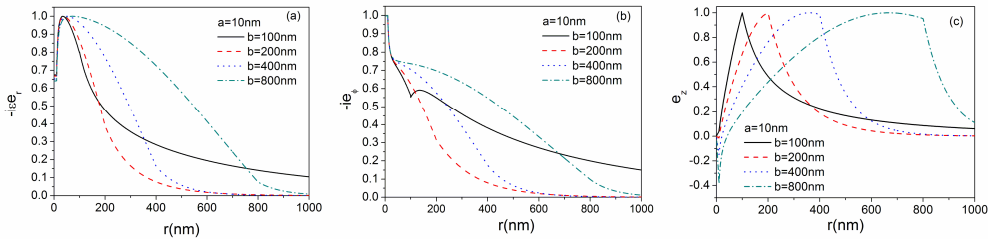

Fig. 3. Electric components of HE_{11} modes of silica SHOF at 633 nm wavelength with different dielectric region radius.

Profiles of power density for two different SHOFs at 633 nm wavelength are shown in Fig. 4, in which the mesh profile stands for propagation field inside the dielectric region, and the gradient profile stands for evanescent fields in air. As can be seen, the SHOF with a=10 nm and b=100 nm leaves a large amount of light guided outside as evanescent waves, while the SHOF with a=100 nm and b=400 nm confines most of the power inside the dielectric region. The intensity in the central hollow region of the SHOF with a=10 nm and b=100 nm has been enhanced though the region is filled with air. The enhanced intensity results from the discontinuity of the electric field at the interface between the hollow region and the dielectric region [9,10]. For the small size of this central air hole, the decay of the evanescent wave within the hole is minimal, and the enhanced field intensities are achieved throughout the hole. The enhanced intensity in the central region may open up the prospect of using these holes as

sites for interacting intense light with materials located within the air region. To clarify the magnitude of enhancement, we define the maximum enhancement factor as the ratio of the maximum power density in the central region of the SHOF and that of the corresponding subwavelength fiber without the central hollow region. In the calculation, we set the power densities of the SHOF and the subwavelength fiber equal at the interface of dielectric region and the outermost air cladding. If b=100 nm, it can be obtained that the maximum enhancement factors are 1.33, 1.26 and 1.13 for the SHOFs with a=10 nm, 20 nm and 40 nm, respectively.
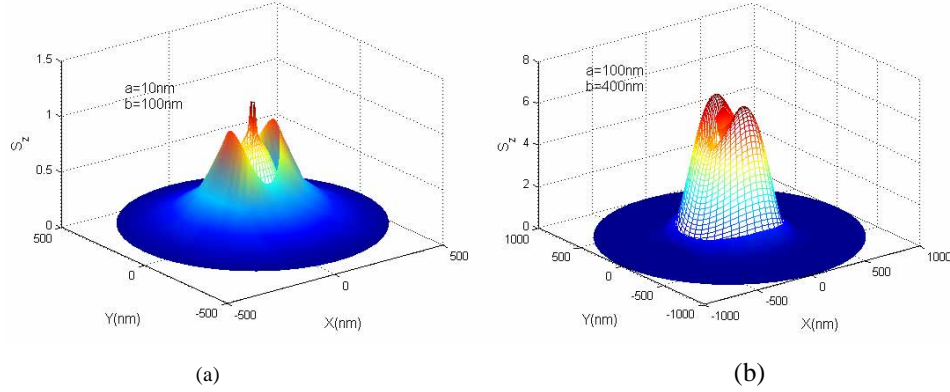

(a)   (b)

Fig. 4. Z-direction power density of silica SHOF with (a) a=10 nm, b=100 nm and (b) a=100 nm, b=400 nm. Mesh, field inside the dielectric region. Gradient, field outside the dielectric region.

To obtain more straight information of the power distribution in the SHOFs, we calculate the fractional power inside the central hollow region (η_1) and the fractional power inside the hollow region and the dielectric region (η_2) defined as following:

$$\eta_1 = \frac{\int_0^a S_{z1}dA}{\int_0^a S_{z1}dA + \int_a^b S_{z2}dA + \int_b^\infty S_{z3}dA},$$

$$\eta_2 = \frac{\int_0^a S_{z1}dA + \int_a^b S_{z2}dA}{\int_0^a S_{z1}dA + \int_a^b S_{z2}dA + \int_b^\infty S_{z3}dA},$$

where $dA=rdrd\Phi$, and S_{z1}, S_{z2} and S_{z3} are the z-components of power density of the central hollow region, the dielectric region and outer cladding, respectively. Calculated η_1 and η_2 as a function of the central hollow region radius (a) are shown in Fig. 5 for SHOF with b=100 nm at 633 nm wavelength. It can be seen clearly that the percentage of the light power in the central hollow region is small for the discussed fiber. With increasing a, the SHOF leaves more light guided outside as evanescent waves.
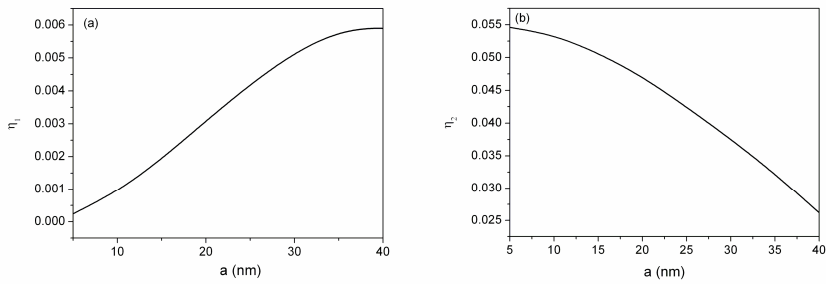
Fig. 5. Fraction power of the fundamental modes inside (a) the central hollow region, and (b) the central and the dielectric region of SHOFs at 633 nm wavelength.

The wavelength-dependent waveguide dispersions of SHOF are shown in Fig. 6. It can be seen clearly that the waveguide dispersions (D_w) of these fibers can be very large comparing with those of weakly guiding fibers. Results also show that, at a particular wavelength, the waveguide dispersion of a SHOF can be made zero, positive or considerably negative when a proper diameter is chosen, as shown in Fig. 6(a). If the central hollow region is enlarged, the dispersion shift is obvious, as shown in Fig. 6(b). Controlling light propagation properties by tailoring waveguide dispersion is used in many fields such as optical communication and nonlinear optics, therefore, these wires present opportunities for achieving enhanced dispersions with reduced sizes.
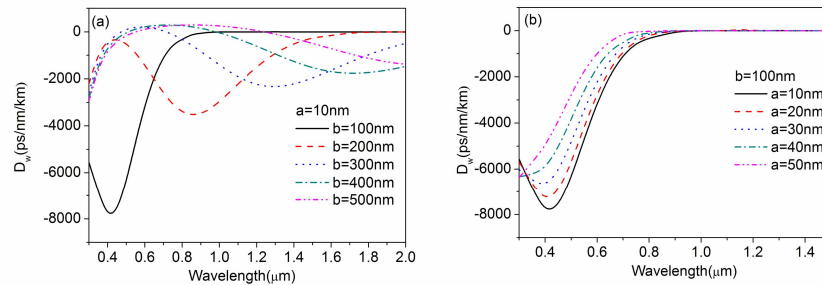

Fig. 6. Wavelength-dependent waveguide dispersion of fundamental modes of SHOF with (a) different *b*; (b) different *a*.

4. Conclusions

We have studied the basic properties of SHOF. We assume the fibers are ideally uniform in terms of the sidewall smoothness and diameter uniformity. By computation, it can be found that the SHOFs have enhanced evanescent field in the outer cladding and local enhanced intensity in the central hollow region. Large waveguide dispersion and large dispersion shift are found for the SHOFs. Compared with large core optical waveguides, the interesting properties may offer opportunities for developing a number of miniaturized high performance and novel photonic devices.

Acknowledgments